Nationaal Lucht- en Ruimtevaartlaboratorium
National Aerospace Laboratory NLR

NLR TP 97082

Comparison of measured and predicted noise of the Brite-EuRam SNAAP advanced propellers

J.B.H.M. Schulten

DOCUMENT CONTROL SHEET

	ORIGINATOR'S REF.		SECURITY CLASS.
	NLR TP 97082 U		**Unclassified**

ORIGINATOR
National Aerospace Laboratory NLR, Amsterdam, The Netherlands

TITLE
Comparison of measured and predicted noise of the Brite-EuRam SNAAP advanced propellers

PUBLISHED IN
AIAA Paper 97-1709 in the Prooceedings of the 3rd AIAA/CEAS Aeroacoustics Conference, Atlanta, Georgia, USA, May 12-14, 1997, by the American Institute of Aeronautics and Astronautics

AUTHORS	DATE	pp	ref
J.B.H.M. Schulten	**970218**	**15**	**14**

DESCRIPTORS
Harmonics
International cooperation
Prediction analysis techniques
Propeller noise
Propellers
Sound pressure
Thrust
Wind tunnel tests

ABSTRACT
In addition to earlier work, in this paper the validation of a lifting surface theory for advanced, single rotation propellers is extended by a comparison with experiments carried out in the Brite-EuRam project SNAAP (Study of Noise and Aerodynamics of Advanced Propellers) of the European Union. In general an acceptable agreement between theory and experiment is found, even at the highest forward speed of Mach = 0.78 where the propeller tip operates supersonically. The inclusion of the suction analogy, which accounts for the leading edge separation vortex, essentially improves the predictions at high aerodynamic loading.

Contents

This page is intentionally left blank.

Comparison of Measured and Predicted Noise of the Brite-EuRam SNAAP Advanced Propellers

Johan B.H.M. Schulten*
National Aerospace Laboratory NLR, 8300 AD Emmeloord, The Netherlands

In addition to earlier work, in this paper the validation of a lifting surface theory for advanced, single rotation propellers is extended by a comparison with experiments carried out in the Brite-EuRam project SNAAP (Study of Noise and Aerodynamics of Advanced Propellers) of the European Union. In general an acceptable agreement between theory and experiment is found, even at the highest forward speed of Mach=0.78 where the propeller tip operates supersonically. The inclusion of the suction analogy, which accounts for the leading edge separation vortex, essentially improves the predictions at high aerodynamic loading.

Introduction

It is well-known that modern advanced propellers can have a fuel economy superior to turbofans, even at high subsonic cruise speeds[1]. However, the noise of propellers is a critical aspect in their application and accurate noise predictions are of great importance to the aircraft industry. As a result a considerable number of prediction schemes has been developed in the past two decades; see the elaborate review article by Metzger & Preisser[2].

In the computation of the aerodynamics and acoustics of advanced propellers, lifting surface methods[3-9] have a special place as they neglect the nonlinear effects in the flow. Although it can be argued that for most operating conditions the flow around a propeller behaves linearly to a large extent[9], experimental validation of this assumption remains necessary. The lifting surface method used in the present study has already been partly validated[7,8] by existing experimental data from literature. However, suitable acoustic data in the high speed regime have been scarce for a long time.

Table 1 SNAAP participants

Alenia	Italy
Aerospatiale	France
Dornier	Germany
Dowty Aerospace Propellers	United Kingdom
Ratier-Figeac	France
Fokker	Netherlands
ONERA	France
CIRA	Italy
NLR	Netherlands
University College Galway	Ireland
Trinity College Dublin	Ireland
IST Lisbon	Portugal
IBK Nuremberg	Germany

*Senior Research Engineer, Aeroacoustics Department, Senior Member AIAA.

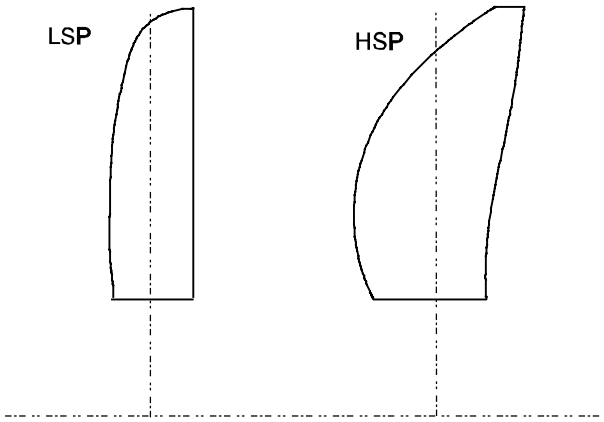

Fig.1 Planforms of SNAAP propellers, the hub is 0.28 tip radius for both

This situation was greatly improved by the experimental data base generated in the EU Brite-EuRam project SNAAP (Study of Noise and Aerodynamics of Advanced Propellers)[10] during the year 1995. In this large scale project, European industries, universities and research institutes [Table 1] cooperated intensively for more than 3 years. This project offered an excellent opportunity for a substantial extension of the validation work done so far.

The present paper discusses the comparison of the experimental results of the SNAAP project with the theoretical predictions of the lifting surface theory. Aerodynamic measurements in the project did not only involve the forces and moments on two different propellers, but also the measurement of the steady and unsteady pressures on the blade surfaces of both propellers. Acoustic measurements were carried out by multiple, in-flow microphone traverses. Furthermore, tests were carried out in two wind tunnels: the high speed regime, relevant for cruise conditions, was tested in the ARA acoustically treated transonic wind tunnel, Bedford, England. The low speed regime, relevant for takeoff and landing, was tested in the open jet of the German-Dutch Wind Tunnel DNW, Noordoostpolder, the Netherlands.

Two 0.9m-diameter, six-bladed model propellers, the blade

planforms of which are shown in Fig.1, were used in the project. The, Dornier designed, *Low Speed Propeller* (LSP) has an unswept trailing edge and a relatively strong blade camber. "Low speed" should not be taken too literally since this propeller is designed for a cruise speed of Mach=0.7. The *High Speed Propeller* (HSP), designed by Ratier-Figeac for a cruise speed of Mach=0.78, shows the characteristics of the NASA propfans[1]: very thin, highly swept blades to cope with a supersonic speed in the tip region. NLR had the responsibility for the structural design and the manufacture of the propeller blades, which were made of carbon fibre composite. A special problem to be solved was the large number of pressure taps be accommodated in the very thin blades. Besides, a large number of miniature transducers for unsteady pressure measurements had to be installed in the blades. The blades perfectly endured the prolonged and intensive wind tunnel testing.
In the present paper first the theoretical modeling will be briefly summarized. This is followed by a discussion on the aerodynamics prediction for both propellers. The low speed acoustic comparison is carried out for the far-field as well as for the near-field, whereas the high speed acoustics are evaluated in the near-field only.

Theoretical modeling

Lifting surface theory

The analysis of the present problem has been described in Refs.7 and 8 in reasonable detail and will only be briefly summarized here for convenience. The lifting surface modeling of a flow problem is based on two assumptions. First, the viscosity of the flow is considered to be small, i.e. the Reynolds number is assumed to be sufficiently high. Secondly, the perturbations of the main flow caused by the presence of the blades are considered to be relatively small. Under these assumptions the governing, i.e. the leading order, flow equations reduce to the linearized Euler equations. Then, upon elimination of the velocity, a non-homogeneous convected-wave equation in the pressure results. The right hand side of this equation consists of two source terms, one of which contains the blade surface pressure distribution and the other the blade thickness distribution.
Following Ref.7 the pressure field of the complete propeller can be expressed as an integral over the blade surfaces. This expression will be used later as the basis to compute the acoustic field. Upon substitution of the pressure field, the momentum equation can be solved for the velocity. The expression of the velocity is then substituted in the boundary condition at the blade surfaces to yield a Fredholm integral equation of the first kind for the unknown pressure jump distribution over the blades.

Numerical Solution

Most lifting surface methods are panel methods in which local basis functions are used for the unknown quantity. To obtain a faster rate of convergence, here global basis functions are used in which the physical behavior of the pressure jump at blade edges is incorporated. If the pressure jump distribution is expressed into a finite series of suitably chosen basis functions, the coefficients in this series are the unknowns. A Galerkin projection method then transforms the integral equation into a finite set of linear equations, which is solved by standard matrix techniques.
Computation of the matrix elements typically takes an hour on a Pentium 133 personal computer. The acoustic calculation for a complete side line takes only a few seconds per harmonic.

Leading edge suction force

As pointed out in Ref.8, the leading edge suction force, a higher order effect which yields zero drag for a plate under an angle of attack in a subsonic, inviscid flow, is not captured by the lifting surface approximation. This force can, however, be recovered by applying locally the two-dimensional potential theory of a semi-infinite plate. From the Blasius theorem it follows that the suction force X is given by

$$X = \frac{\pi}{4}\frac{c}{2}\frac{1}{(\cos\Lambda)^2}\lim_{x\downarrow 0}\left[\sqrt{x}\,\Delta C_p(x)\right]^2 \qquad (1)$$

where Λ is the local sweep angle of the leading edge and x denotes a local coordinate (scaled on the local semi-chord) normal to the leading edge and tangent to the helical surface. It is well known[11,12], however, that for the sharp leading edge of airfoils of advanced propellers a local separation occurs at the suction side which develops into a leading edge vortex. As shown for wings by Polhamus[13] and Lamar[14] the effect of this vortex is to rotate the leading edge suction force over 90 degrees to the suction side of the blade. This effect is the so-called leading edge suction analogy which has been included in the present theory.

Aerodynamic results

LSP

Blade pressures In Fig.2 the local blade lift coefficient of the LSP is given for a forward Mach number of 0.7, an advance ratio of 4.036 and a blade angle of 61.8 deg (at 75% span). In this figure the experimental lift coefficients were obtained from integrating the measured pressures. It is readily observed that the agreement between measured and computed results is encouraging.
In Fig.3 the local pressure jump distribution is presented in terms of ΔC_p for a spanwise location of 70%. The theory confirms the negative leading edge suction peak along the span for this condition, which complies with the fairly high camber of this propeller.
Thrust and power Figs.4 and 5 give the thrust and shaft power at a forward Mach number of 0.7 for 2 blade setting angles. A slight overprediction of the aerodynamic loading is found for the lowest blade angle (54.9 deg) but the higher angle (61.8 deg) results are in agreement with the measured data.

HSP

As an example, in Figs.6 and 7 the thrust and shaft power of the HSP at a forward Mach number of 0.78 is presented. The good agreement is observed with only a slight underprediction of the highest loading condition. It can be concluded that the agreement in the high speed range is much better than found

in Ref.8 for the eight-bladed NASA propfan SR7a. Probably this is a consequence of the thinner root blade section and the lower number of blades (6) of the HSP.

Acoustic results

Parallel to the aerodynamic measurements, a vast amount of acoustic data was gathered during the test program. In this section, part of these results will be used for a comparison with the computed lifting surface results. Angle of attack effects will not be considered.

Low speed

A large series of tests was carried out to investigate the far-field acoustic behavior of the propellers at takeoff and landing conditions in the DNW. For the present validation a number of typical cases was selected. All measurements used here were taken at a Mach number of 0.2 along an in-flow side line at a distance of 5.551 tip radii from the propeller axis.

LSP In Fig.8 a typical 1st harmonic sound pressure level of the LSP is presented. It appears that application of the suction analogy is needed to achieve a good fit with the measured data. For the second harmonic in Fig.9 the discrepancy with the experimental results is not completely removed by the suction analogy. However, the rather similar case presented in Figs.10-12 shows an acceptable agreement. This continues to be the case if the blade angle is reduced by 3 degrees, as is shown in Figs.13 and 14.

HSP For the HSP a highly loaded condition typical for takeoff is shown in Figs.15-17. The geometric angle of attack at 78 % span (α_{78}) is 13.1 degrees. Although the rotated suction reduces the discrepancy with the measured data, a considerable gap of about 4 dB remains in the 1st harmonic peak level. Comparing this result with an axial traverse taken in the near-field in the ARA tunnel for a higher loading (α_{78}= 16.9 deg.) at the same Mach number in Figs.18-20, we observe an even larger discrepancy in the order of 8 dB. As shown in Figs.21-23 a substantial reduction of rotational speed (Advance ratio J from 1.02 to 1.30) and consequently of loading restores the agreement between measurement and prediction to some extent. If blade deflection is excluded as a possible cause of this large discrepancy, it could be that more nonlinear effects than just the suction analogy have to be included to obtain a better prediction at high loading.

High speed

All high speed acoustic measurements used here are along a side line at a relative radius of r=1.22. The suction analogy is included in all theoretical results presented.

LSP Fig.24 presents the 1st harmonic sound pressure level of the LSP for a forward Mach number of 0.6. Figs.25 and 26 present the 2nd and 3rd harmonics. The agreement with the experiments is quite acceptable for this case despite a slight underprediction for all harmonics. As shown in Figs.27-29 this underprediction is more obvious at a Mach number of 0.7. Note that this is the case for which the computed aerodynamics compared favorably with the measurements.

The first four harmonics of the radial pressure in the propeller plane (x=0.0) are presented in Fig.30. Up to a relative radius of about r=1.5 the measured radial decrease agrees fully with the (free space) theory. At larger distances, wall interference effects inevitably result in a deviation from the computed free space acoustic field. Another check on the anechoic behavior of the tunnel is given in Fig.31 which presents the results of a circumferential traverse over 60 degrees in the propeller plane. Since the test section has a rectangular shape, wall refections are obviously weak at this radius.

HSP Although it remains useful to consider unswept propellers like the LSP, the basic motivation of the present validation is a comparison with a real propfan like the HSP.

Figs. 32-34 show the results for an intermediate Mach number of 0.5. With only a slight underprediction the agreement of the theory with experiments is quite good for this case. This can not be said of the results obtained at a Mach number of 0.74 in Figs.35-37. Here, the peak level is underpredicted by 4 dB for the 1st harmonic and by some 8 dB for the 3rd. Strong wall interference and reflections from the microphone traverse system seem to responsible for unpredictable off-peak behavior.

A further increase in Mach number to M=0.78 does not necessarily degrade the prediction as is shown in Figs.38-40. Admittedly, the aerodynamic loading is somewhat lower than in the previous case.

Finally, results of the highest loaded case for this Mach number (α_{78}= 6.9 deg., see also Figs.6 and 7) are shown in Figs.41-43. The first harmonic has an impressive peak level of more than 160 dB. The predictions are remarkably close to the experimental results, especially for the 2nd and 3rd harmonic. Note that the blade tip region with a helical tip Mach number of 1.08 operates in the supersonic regime.

Concluding remarks

In addition to earlier validations, in this paper the validation of a lifting surface theory for advanced, single rotation propellers is extended by a comparison with the experiments carried out in the EU Brite-EuRam project SNAAP (Study of Noise and Aerodynamics of Advanced Propellers). From this comparison the following conclusions result.

The blade pressure jump distribution is in good agreement with the lifting surface predictions, at least for acoustic purposes.

For both the LSP and HSP the measured thrust and power are accurately predicted, also for high Mach numbers which was not the case for the NASA SR7a propfan.

In the low speed regime the LSP 1st harmonic level is accurately predicted if the suction analogy is taken into account. The higher harmonics sometimes tend to be slightly underpredicted. The highly loaded HSP case investigated shows an overall underprediction, especially in the near field.

In the Mach number range from 0.5 to 0.7 in most cases the measured acoustic data agree satisfactorily with the predicted values. For the higher Mach numbers from 0.74 to 0.78, however, some underprediction of the peak level is the rule. At these Mach-numbers the off-peak behavior can not easily be validated because of the presence of wall interference and spurious reflections from the microphone traverse system.

Acknowledgement

The permission given by the SNAAP partners to use the experimental results is gratefully acknowledged. The development of the theoretical method was supported by the Netherlands Agency for Aerospace Programs, NIVR.

References

[1]Hager, R.D., Vrabel, D., "Advanced Turboprop Project," NASA SP-495, 1988.

[2]Metzger, F.B., Preisser, J.S., "A History of Propeller Tone Noise Prediction Methodology 1919 to 1994," CEAS/AIAA Paper 95-006, June 1995.

[3]Hanson, D.B., "Unified Aeroacoustic Analysis for High Speed Turboprop Aerodynamics and Noise. *Volume I - Development of Theory for Blade Loading, Wakes, and Noise*," NASA CR 4329, March 1991.

[4]Hwang, Ching-Chywan, "Propfan Supersonic Panel Method Analysis and Flutter Predictions," Ph.D. Thesis, Purdue University, May 1990.

[5]Chen, S.H., "Prediction of Periodic Loadings on a Single Rotation Propfan with Off-Axis Inflow," *Journal of Propulsion and Power*, Vol.8, No.1, Jan.-Feb. 1992, pp. 144-150.

[6]Lohmann, D., "Prediction of Ducted Radiator Fan Aeroacoustics with a Lifting Surface Method," DGLR/AIAA Paper 92-02-098, May 1992.

[7]Schulten, J.B.H.M., "Effects of Asymmetric Inflow on Near-Field Propeller Noise," *AIAA Journal*, Vol.34, No.2, Feb. 1996, pp. 251-258.

[8]Schulten, J.B.H.M., "Advanced Propeller Performance Calculation by a Lifting Surface Method," *Journal of Propulsion and Power*, Vol.12, No.3, May-June 1996, pp.477-485.

[9]Schulten, J.B.H.M, "Sound Generation by Ducted Fans and Propellers as a Lifting Surface Problem," Ph.D. Thesis, University of Twente, Enschede, The Netherlands, Feb. 1993.

[10]Commission of the European Communities, "Synopses of Current Aeronautic Projects 1993," EUR 15292, Brussels, 1993.

[11]Stefko, G.L., Rose, G.E., Podboy, G.G., "Wind Tunnel Performance Results of an Aeroelastically Scaled 2/9 Model of the PTA Flight Test Prop-Fan," AIAA Paper 87-1893, June 1987.

[12]Hanson, D.B., "Propeller Noise Caused by Blade Tip Radial Forces," AIAA Paper 86-1892, July 1986.

[13]Polhamus, E.C., "A Concept of the Vortex Lift of Sharp-Edge Delta Wings Based on a Leading-Edge-Suction Analogy," NASA TN D-3767, 1966.

[14]Lamar, J.E., "Prediction of Vortex Flow Characteristics of Subsonic and Supersonic Speeds," *Journal of Aircraft*, Vol.13, No. 7, July 1976, pp. 490-494.

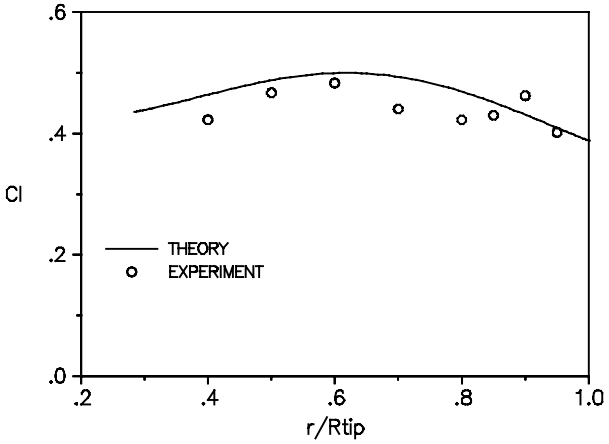

Fig.2 LSP spanwise lift coefficient, β_{75}=61.8 deg, *M*=0.70, *J*=4.036, (ARA case 9).

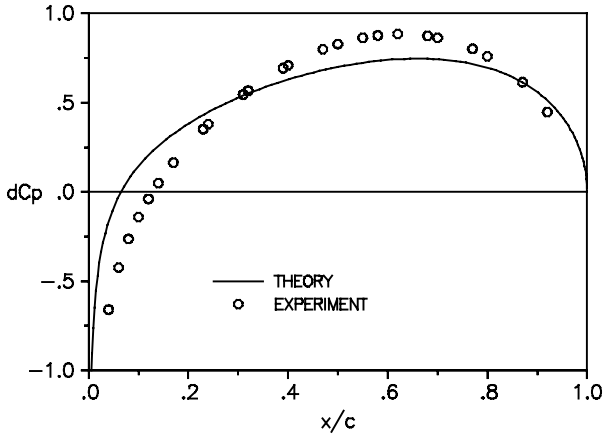

Fig.3 LSP chordwise pressure jump distribution, *r*=0.7, conditions as in Fig.2.

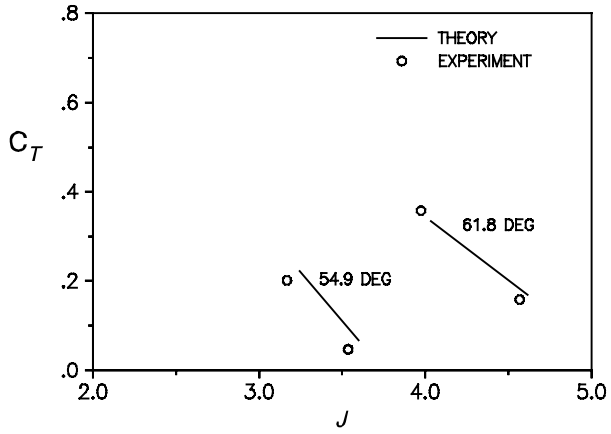

Fig.4 LSP thrust, M=0.7, 2 blade angles.

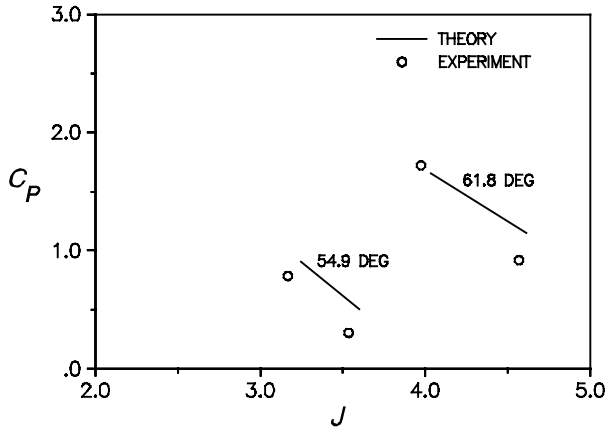

Fig.5 LSP shaft power, M=0.7, 2 blade angles.

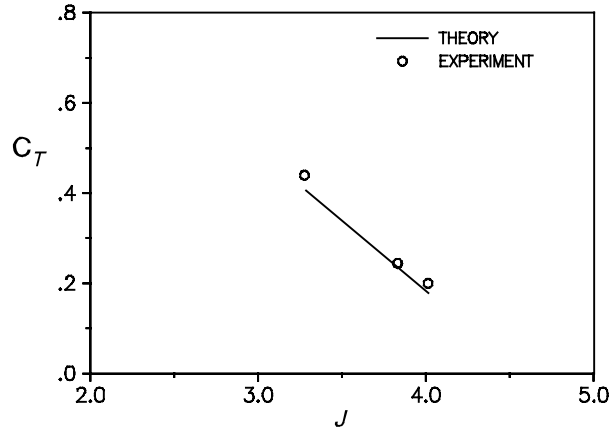

Fig.6 HSP thrust, M=0.78, β_{75}=61.1 deg.

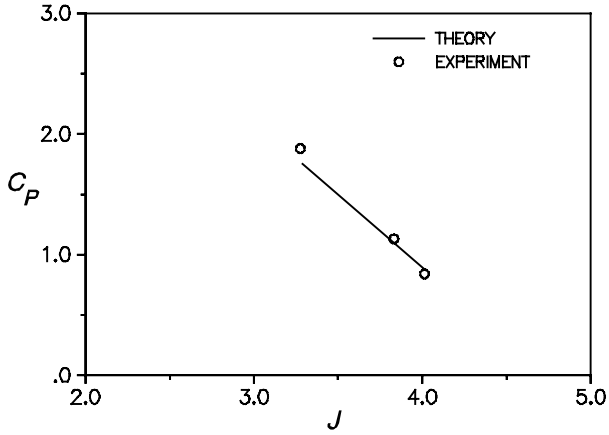

Fig.7 HSP shaft power, M=0.78, β_{75}=61.1 deg.

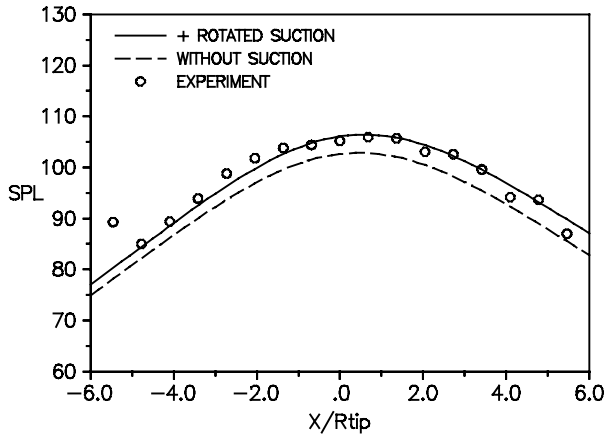

Fig.8 LSP sound level 1st harmonic, β_{75}=41.1 deg, M=0.199, J=1.161, r=5.551 (Mic.2), (DNW case 1).

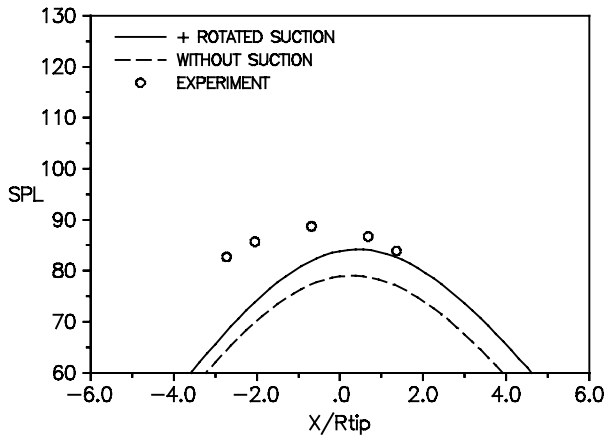

Fig.9 2nd harmonic, conditions as in Fig.8.

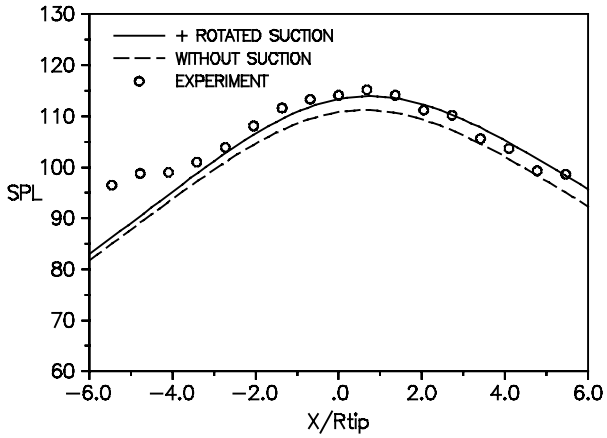

Fig.10 LSP sound level 1st harmonic, β_{75}=39.0 deg, *M*=0.198, *J*=1.012, *r*=5.551.

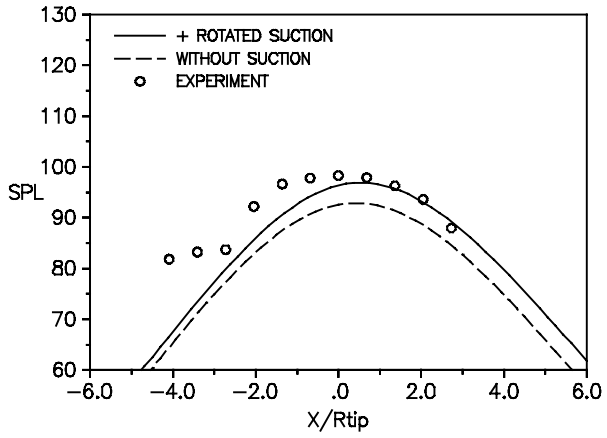

Fig.11 2nd harmonic, conditions as in Fig.10.

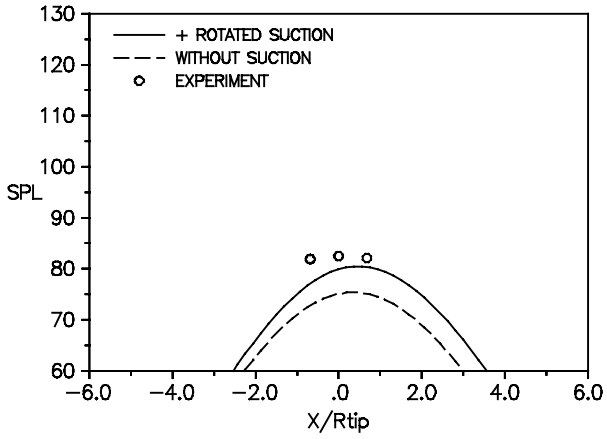

Fig.12 3rd harmonic, conditions as in Fig.10.

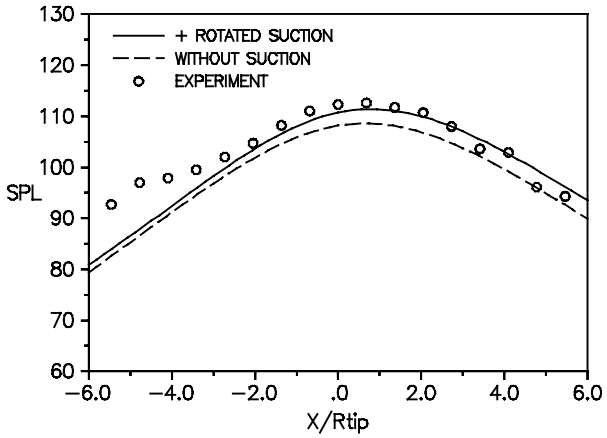

Fig.13 LSP sound level 1st harmonic, β_{75}=36.0 deg, *M*=0.199, *J*=1.013, *r*=5.551, (DNW case 7).

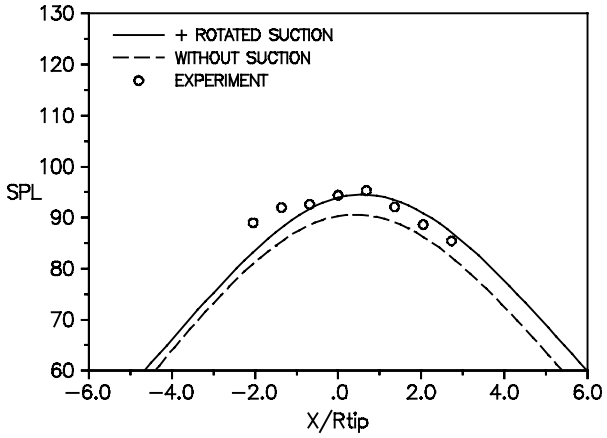

Fig.14 2nd harmonic, conditions as in Fig.13.

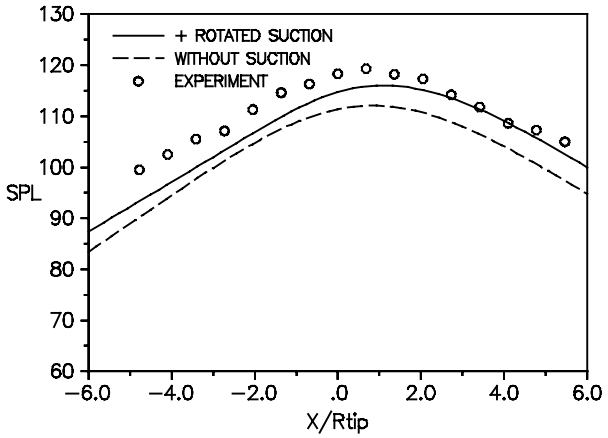

Fig.15 HSP sound level 1st harmonic, β_{75}=35.0 deg, *M*=0.199, *J*=0.942, *r*=5.551, (DNW case 8).

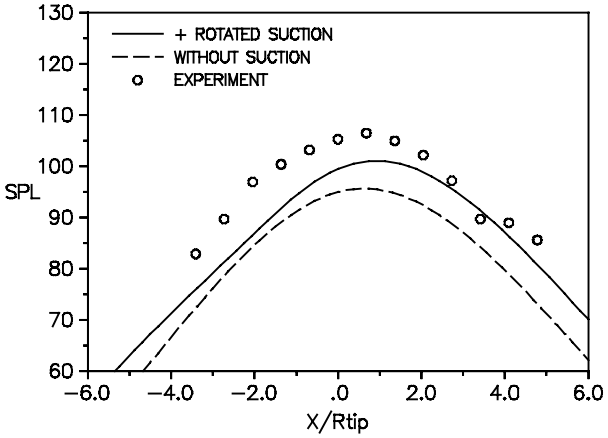

Fig.16 2nd harmonic, conditions as in Fig.15.

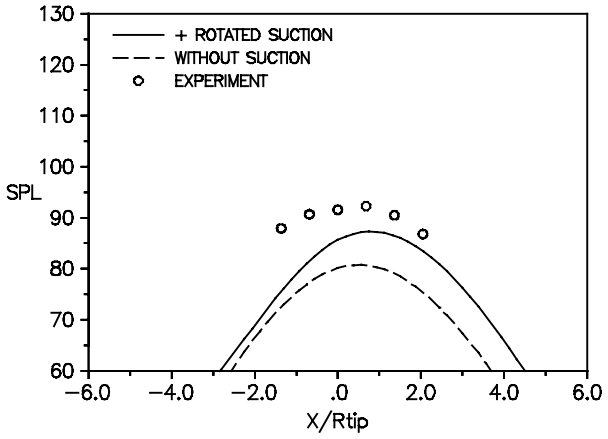

Fig.17 3rd harmonic, conditions as in Fig.15.

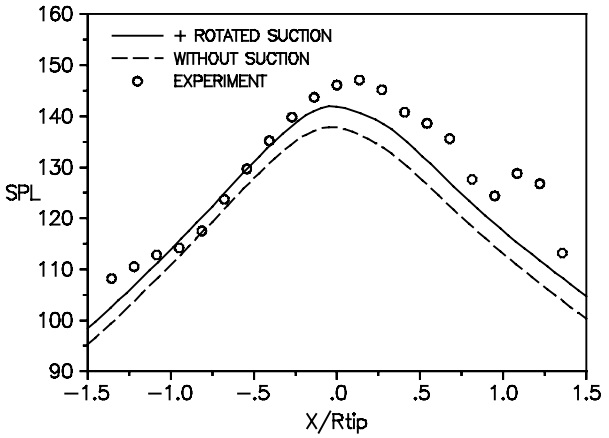

Fig.18 HSP sound level 1st harmonic, β_{75}=40.4 deg, *M*=0.201, *J*=1.020, *r*=1.22 (Mic.7).

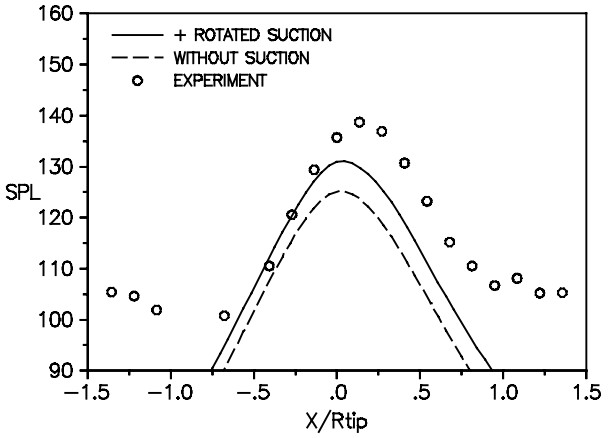

Fig.19 2nd harmonic, conditions as in Fig.18.

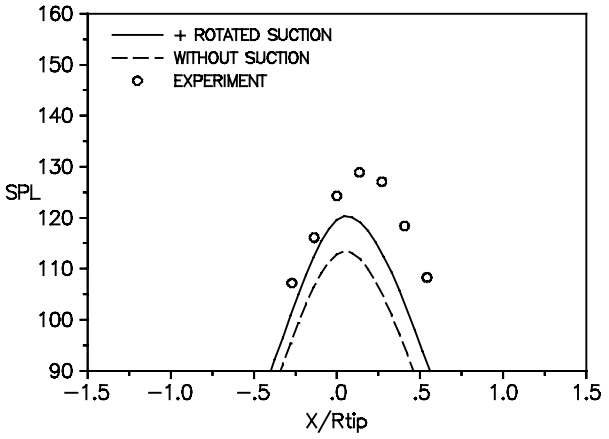

Fig.20 3rd harmonic, conditions as in Fig.18.

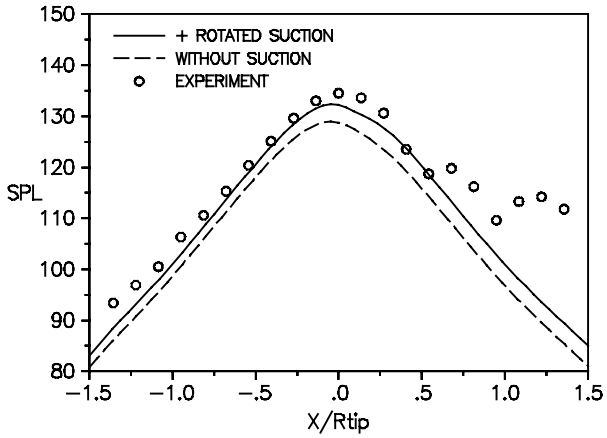

Fig.21 HSP sound level 1st harmonic, β_{75}=40.4 deg, *M*=0.200, *J*=1.303, *r*=1.22.

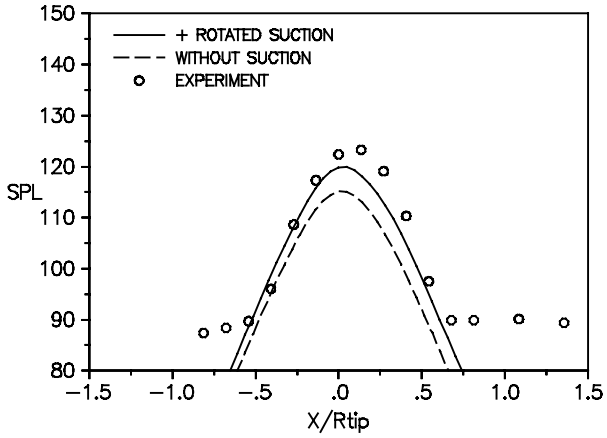

Fig.22 2nd harmonic, conditions as in Fig.21.

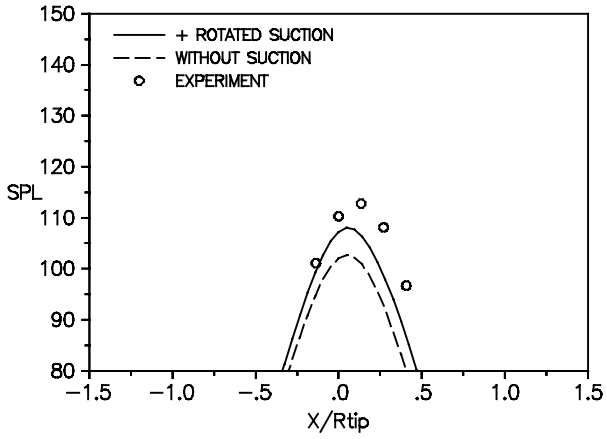

Fig.23 3rd harmonic, conditions as in Fig.21.

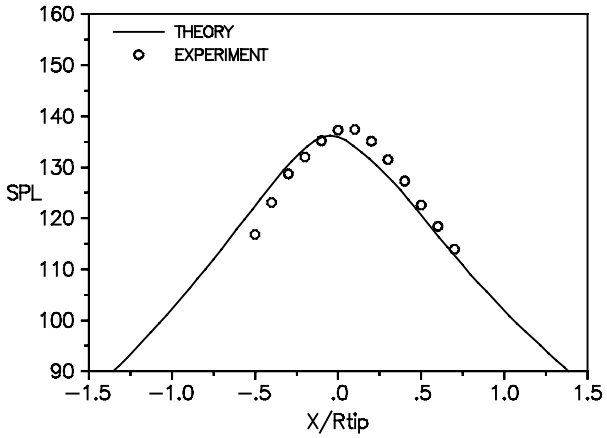

Fig.24 LSP sound level 1st harmonic, β_{75}=61.8 deg, *M*=0.599, *J*=4.042, *r*=1.22, (ARA case 11).

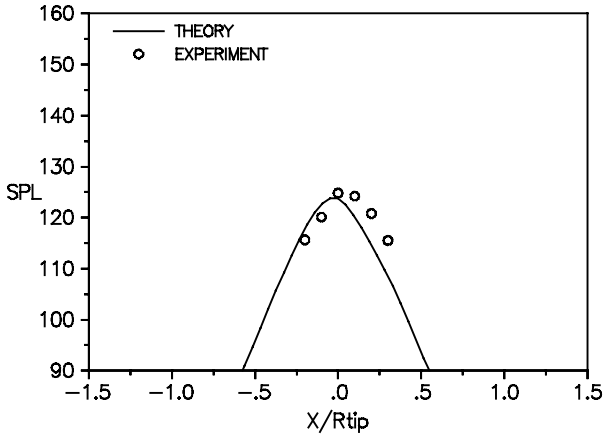

Fig.25 2nd harmonic, conditions as in Fig.24.

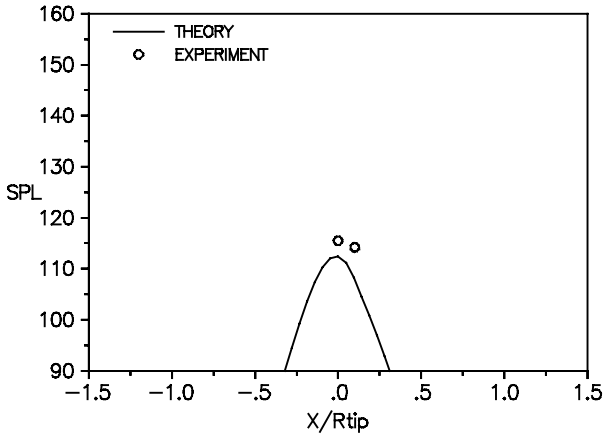

Fig.26 3rd harmonic, conditions as in Fig.24.

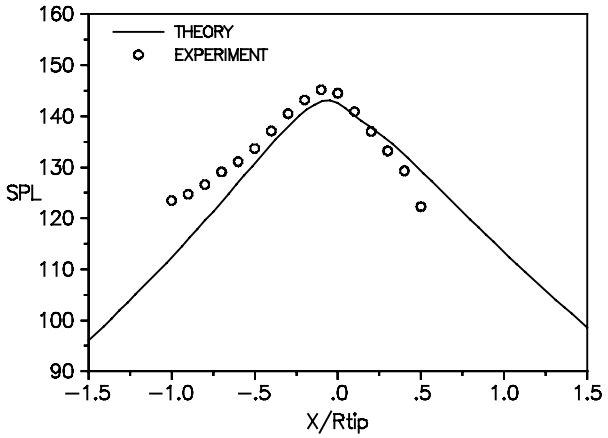

Fig.27 LSP sound level 1st harmonic, β_{75}=61.8 deg, *M*=0.70, *J*=4.036, *r*=1.22, (ARA case 7).

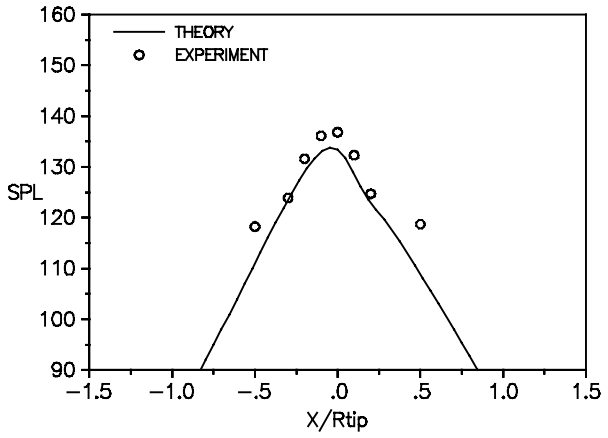

Fig.28 2nd harmonic, conditions as in Fig.27.

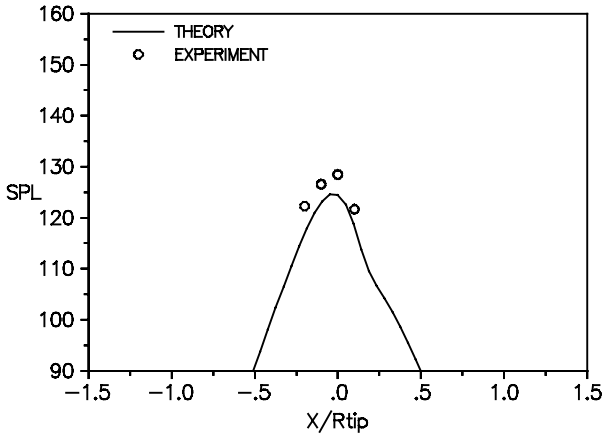

Fig.29 3rd harmonic, conditions as in Fig.27.

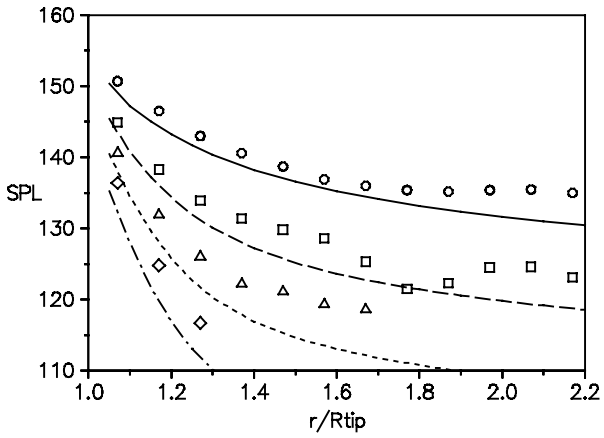

Fig.30 Radial traverse LSP, *x*=0.0, harmonics 1-4, conditions as in Fig.27.

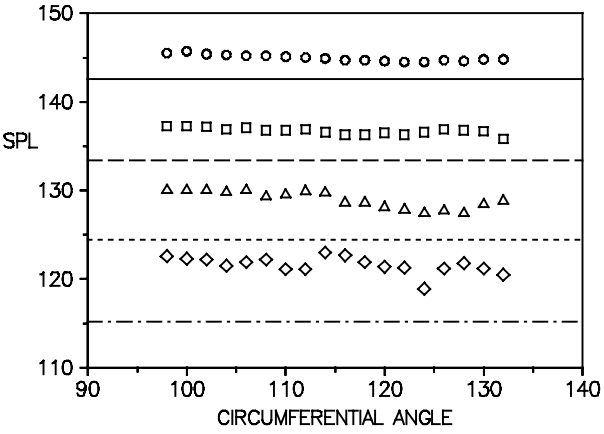

Fig.31 Circumferential traverse LSP, *x*=0.0, harmonics 1-4, conditions as in Fig.27, r=1.22.

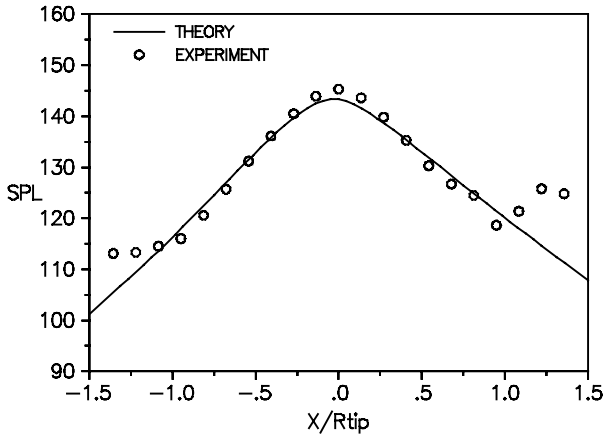

Fig.32 HSP sound level 1st harmonic, β_{75}=51.6, *M*=0.501, *J*=2.346, *r*=1.22, (ARA case 5).

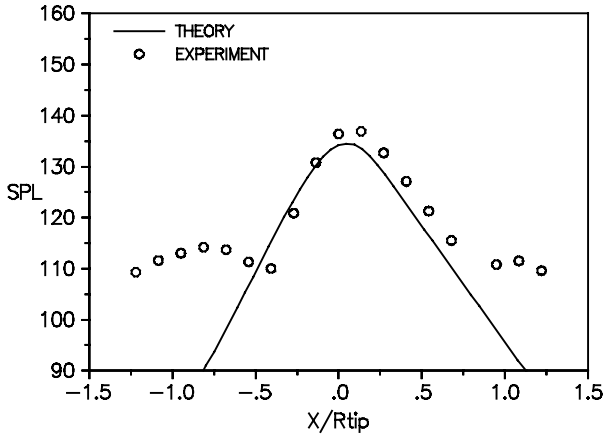

Fig.33 2nd harmonic, conditions as in Fig.32.

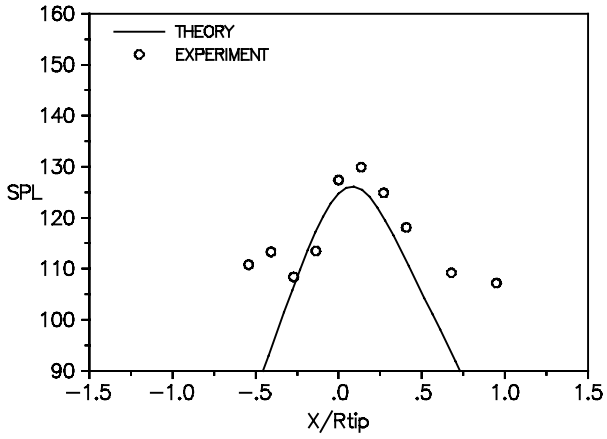

Fig.34 3rd harmonic, conditions as in Fig.32.

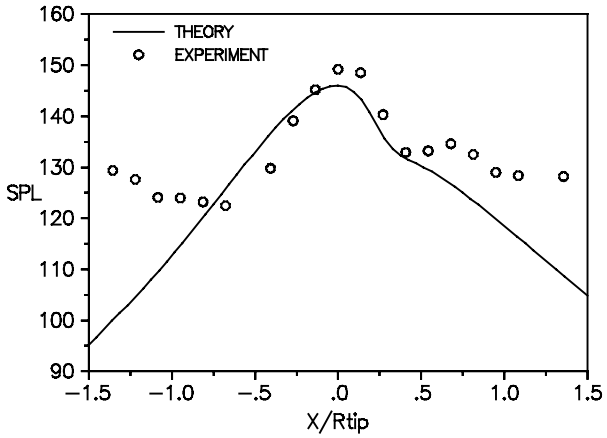

Fig.35 HSP sound level 1st harmonic, β_{75}=61.1, *M*=0.735, *J*=3.809, *r*=1.22, (ARA case 4).

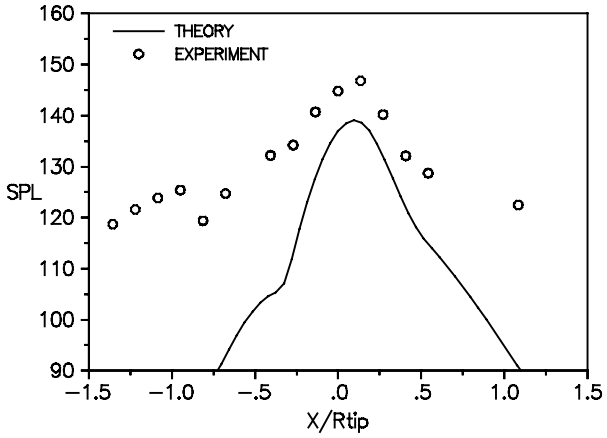

Fig.36 2nd harmonic, conditions as in Fig.35.

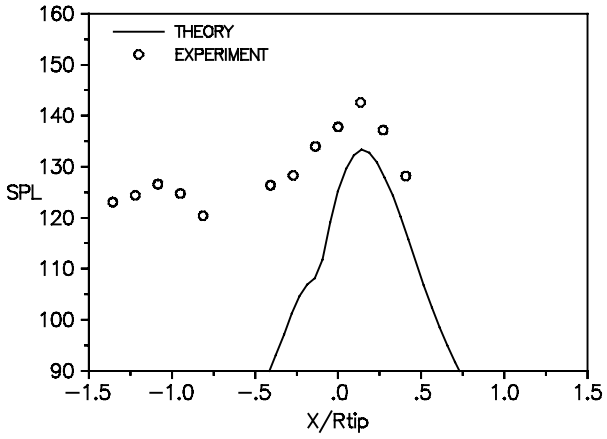

Fig.37 3rd harmonic, conditions as in Fig.35.

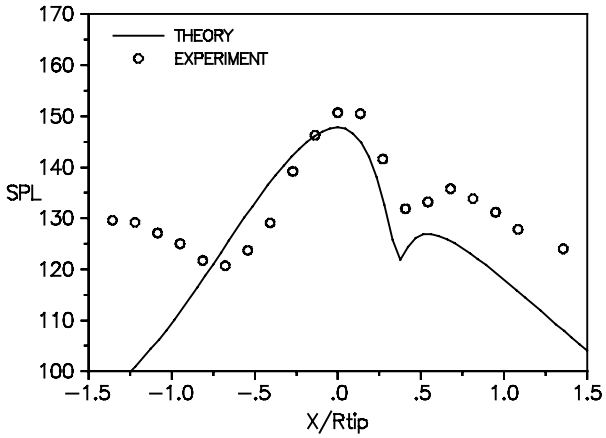

Fig.38 HSP sound level 1st harmonic, β_{75}=61.1, *M*=0.780, *J*=4.016, *r*=1.22, (ARA case 2).

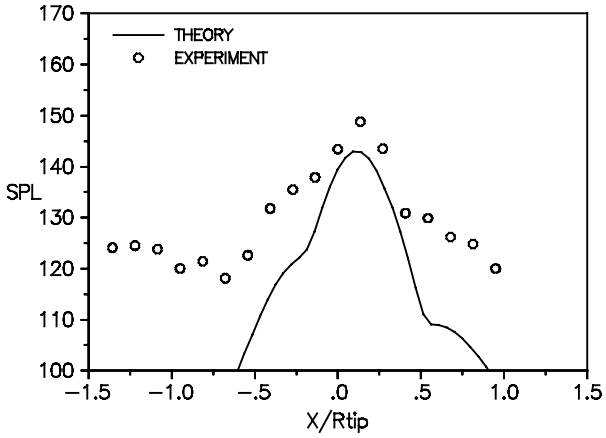

Fig.39 2nd harmonic, conditions as in Fig.38.

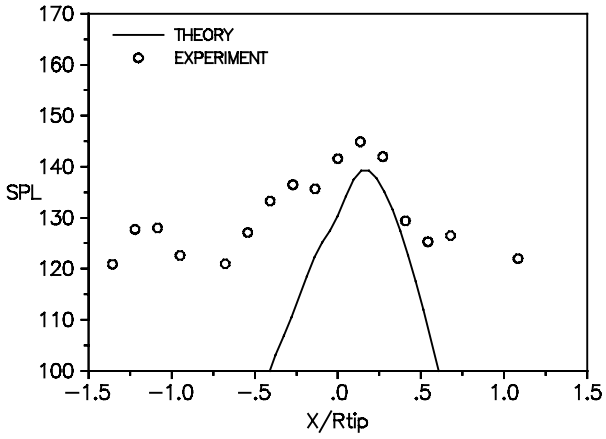

Fig.40 3rd harmonic, conditions as in Fig.38.

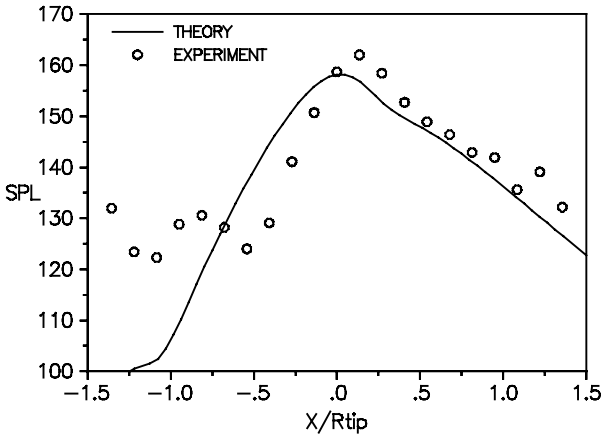

Fig.41 HSP sound level 1st harmonic, β_{75}=61.1, *M*=0.781, *J*=3.287, *r*=1.22, (ARA case 1).

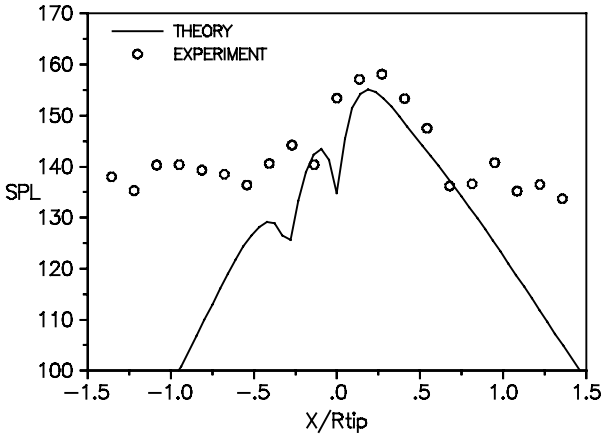

Fig.42 2nd harmonic, conditions as in Fig.41.

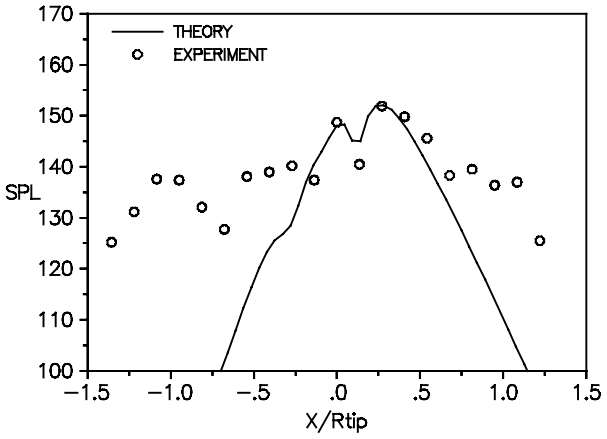

Fig.43 3rd harmonic, conditions as in Fig.41